Infrared Spectroscopy of Neutral Water Dimer Based on a Tunable Vacuum Ultraviolet Free Electron Laser

Bingbing Zhang,[#] Yong Yu,[#] Zhaojun Zhang,[#] Yang-Yang Zhang,[#] Shukang Jiang, Qinming Li, Shuo Yang, Han-Shi Hu, Weiqing Zhang, Dongxu Dai, Guorong Wu, Jun Li,* Dong H. Zhang,* Xueming Yang,* and Ling Jiang*

ACCESS | Metrics & More | Article Recommendations | SI Supporting Information

ABSTRACT: Infrared (IR) spectroscopy provides detailed structural and dynamical information on clusters at the fingerprint level. Herein, we demonstrate the capability of a tunable vacuum ultraviolet free electron laser (VUV-FEL) for selective detection of a wide variety of neutral water clusters and for recording the size-dependent IR spectra. The present technique does not require the presence of an ultraviolet chromophore or a dipole moment and is generally applicable for IR spectroscopy of neutral clusters free from confinement. To show the features of our technique, we report here the IR spectra of neutral water dimer in the OH stretch region, providing benchmarks for theoretical study of the accurate description of hydrogen bonding structures involved in liquid water and ice. Quantum mechanical calculations on a 12-dimensional ab initio potential energy surface are utilized to simulate the anharmonic vibrational spectra of water dimer. These results help to resolve the controversy of the exact vibrational assignment of each band feature of the water dimer.
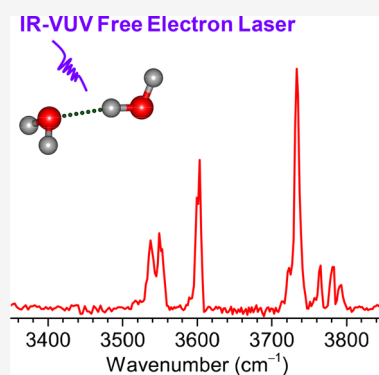
Clusters consisting of a few to hundreds of atoms exhibit interesting size-dependent properties and are the bridge between molecules and the condensed phase bulk.[1] Optical spectroscopy of gas-phase clusters provides detailed structural and dynamical information that is difficult to extract from bulk measurements. Over the past several decades, enormous efforts were devoted to the spectroscopic study of charged clusters, which allow easy size selection and detection. In contrast, neutral clusters have presented major experimental challenges, because the absence of a charge makes for difficult size selection and detection. Currently, various spectroscopic techniques have been developed to study the structure and dynamics of neutral clusters, such as Fabry−Perot cavity pulsed Fourier transform microwave spectroscopy,[2] IR-molecular-beam spectroscopy,[3,4] scattering analysis of cluster beams,[5] helium-droplet evaporation spectroscopy,[6] far-IR spectroscopy,[7] population-modulated attachment spectroscopy,[8] and broadband chirped-pulse Fourier transform microwave spectroscopy,[9] although their applications are practically restricted to small-sized clusters because of the lack of intrinsic size-selectivity in their approaches. Size-specific IR spectra of neutral clusters can be achieved by infrared-ultraviolet (IR-UV) double-resonance spectroscopy,[10] in which the cluster of interest is required to have a chromophore in the UV or visible region for electronic transition measurements to detect the population transfer. This prerequisite thus limits the general application of this technique.

Infrared-vacuum ultraviolet (IR-VUV) is an alternative scheme for structural characterization of neutral clusters,[11−13]

in which VUV one-photon ionization does not require a chromophore (intermediate state) and the cluster can be softly ionized without extensive fragmentations while the VUV photon energy is near the ionization threshold. However, current IR-VUV spectroscopy of neutral clusters is limited by the lack of a tunable intense laser in the entire VUV region. Recently, we have developed the Dalian Coherent Light Source (DCLS) facility,[14] which delivers a VUV free electron laser (FEL) with a continuously tunable wavelength region between 50 and 150 nm and high pulse energy. Inasmuch as clusters with different sizes have different ionization energies, the tunable VUV-FEL light paves the way for selectively ionizing a given neutral cluster free of confinement, thus facilitating realization of their size selectivity. This unique VUV-FEL facility makes it possible to study the IR spectroscopy of confinement-free, neutral clusters via the IR-VUV scheme.

In this Letter, we have chosen the well-studied water dimer as an example to demonstrate the capability of using our VUV-FEL light source to detect the infrared spectra of a wide range of neutral clusters and molecules. The water cluster is considered here because of its central role in scientific disciplines ranging from geology to astronomy to biology.[15−26]

The water dimer is a prototype system for the study of the cooperative hydrogen bond (HB) in liquid water,[3,4,15,27−30] which has proven to be difficult to adequately capture through bulk experiments or theory.[31] Experimental work on the water dimer was reviewed by Saykally and co-workers.[32,33] For comparison, a brief summary for previous gas-phase IR spectra is given in Figure S1b−f in the Supporting Information.[4,15,28,34,35] However, the exact vibrational assignment of each band feature remains controversial (Table S1).[32,33]

Here, we report the IR spectra of the water dimer based on soft near-threshold photoionization using our tunable VUV-FEL light source. The experiments were performed using the IR-VUV spectroscopy apparatus (Figure S2). Briefly, neutral water clusters were produced by supersonic expansions of water seeded in helium using a high-pressure pulsed valve. The neutral water clusters were ionized by one-photon absorption of VUV-FEL light and mass-analyzed in a reflectron time-of-flight mass spectrometer. The tunable IR light pulse was introduced at about 30 ns prior to the VUV-FEL pulse in a crossed manner. When the IR laser frequency was resonant with a vibrational transition of a selected neutral cluster, vibrational predissociation caused the depletion of the VUV ionization signal of the neutral cluster. The IR spectra of this size-selected neutral cluster can then be recorded by monitoring the depletion of the signal intensity for a specific water cluster as a function of IR wavelength.

Figure 1 shows the mass spectra of water clusters ionized at different VUV-FEL wavelengths. Two series of water clusters
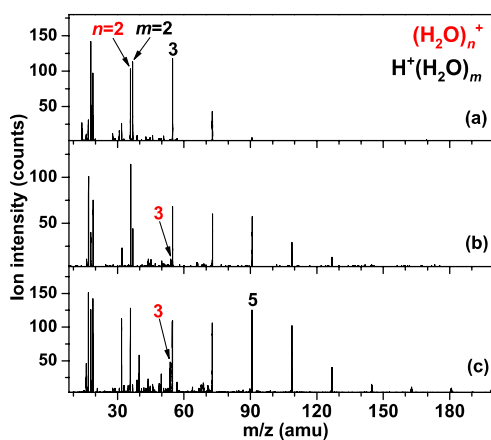
Figure 1. Time-of-flight mass spectra of the cations produced from the VUV-FEL single-photon ionization process: (a) $\lambda_{VUV\text{-}FEL}$ = 98.10 nm, (b) $\lambda_{VUV\text{-}FEL}$ = 108.00 nm, and (c) $\lambda_{VUV\text{-}FEL}$ = 110.00 nm.

ions are observed: one unprotonated $(H_2O)_n^+$ and the other protonated $H^+(H_2O)_n$. Photoionization of neutral water clusters creates the unprotonated $(H_2O)_n^+$ cations, which could undergo very fast intracluster charge redistribution on the subpicosecond time scale.[36,37] The most thermodynamically and kinetically favorable reaction pathway is proton transfer and subsequent OH loss (reaction 1). As a result, the protonated water clusters are dominated in the mass spectra.[37,38] Previous studies indicate that the loss of OH from $(H_2O)_n^+$ (reaction 1) is much less endothermic than that of H_2O (reaction 2).[38] For example, at the MP2/aug-cc-pVDZ level, the loss of OH and H_2O from $(H_2O)_2^+$ is calculated to be endothermic by 89.2 and 179.6 kJ/mol, respectively. Thus, a relatively slow water molecule evaporation process (reaction 2)[36−38] could be suspended by reducing the excess energy

from the ionization via the fine-tuning of the wavelength and pulse energy of VUV-FEL.

$$(H_2O)_n^+ \rightarrow H^+(H_2O)_{n-1} + OH \tag{1}$$

$$(H_2O)_n^+ \rightarrow (H_2O)_{n-1}^+ + H_2O \tag{2}$$
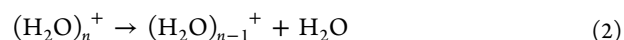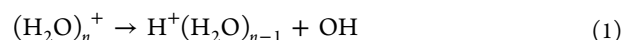
Various experimental conditions (i.e., the wavelength and pulse energy of VUV-FEL, concentration of water/helium mixture, and stagnation pressure) were optimized to maximize the signal of the $(H_2O)_n^+$ cluster of interest and minimize the contribution from the larger cluster. At 98.10 nm (12.64 eV), the unprotonated $(H_2O)_2^+$ cluster is clearly observed (Figure 1a). The mass spectral signal of $(H_2O)_3^+$ is observable at 108.00 nm (11.48 eV) (Figure 1b) and remarkably enhanced at 110.00 nm (11.27 eV) (Figure 1c). Mass spectra of water clusters at different VUV-FEL pulse energies reveal high sensitivity of ionization (Figure S3). For instance, trace species from the background were readily detected using the VUV-FEL with 21 μJ/pulse energy, where the pressure of the ionization chamber was about 5 × 10^{-6} Pa (Figure S3d). Therefore, IR spectra of size-selected neutral $(H_2O)_2$ can be obtained by monitoring ion signal intensities of the unprotonated $(H_2O)_2^+$ cations at 98.10 nm. The IR-VUV scheme of neutral $(H_2O)_2$ is free from spectral contamination because the IR excited water clusters dominantly dissociate into the monomer and protonated cluster cation mass channels in the VUV photoionization process.[39] This is a special feature of our approach, especially because the system under consideration is confinement-free.

The HB dissociation energy of the water dimer is measured as 13.2 kJ/mol,[40,41] indicating that, assuming internally cold complexes, the absorption of one IR photon around 3700 cm^{-1} (~44.3 kJ/mol) is sufficient for overcoming the dissociation limit. IR power dependence of the signal is measured to ensure that the predissociation yield is linear with photon flux. Figure 2 shows the IR laser power dependence for IR spectra of the water dimer at 98.10 nm. The band positions are given in Table 1.
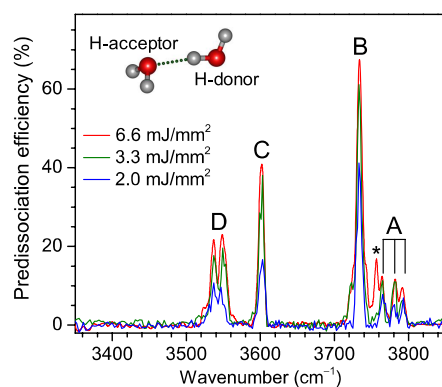
Figure 2. IR laser power dependence for IR spectra of $(H_2O)_2$ measured with the VUV-FEL wavelength of 98.10 nm. The OH stretch fundamentals assigned to antisymmetric OH stretch of the proton acceptor (A), free OH stretch of the proton donor (B), symmetric OH stretch of the proton acceptor (C), and hydrogen-bonded OH stretch of the proton donor (D) are labeled. The band labeled with "*" (3757 cm^{-1}) might arise from a combined or overtone excitation (see the text). The structure of the water dimer is shown in the inset.
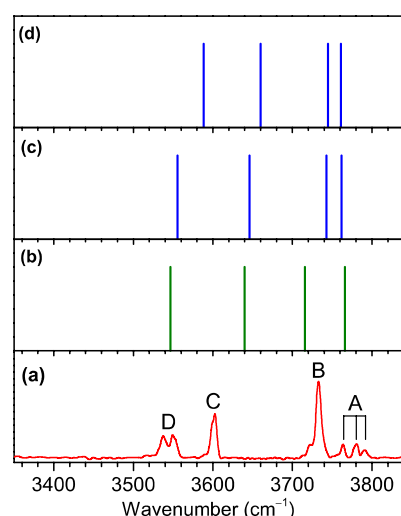
Table 1. Experimental IR Band Positions (cm^{-1}), 12-Dimensional Potential Energy Surface Anharmonic Vibrational Frequencies (12D), MP2/aug-cc-pVTZ (MP2) and CCSD(T)/aug-cc-pVTZ (CCSD(T)) Harmonic Frequencies, and Band Assignments for the Water Dimer

label	exptl	12D	MP2	CCSD(T)	assignment
A	3792	3766	3762	3761	antisymmetric OH stretch of the proton acceptor
	3780				
	3764				
B	3732	3716	3743	3745	free OH stretch of the proton donor
C	3603	3640	3646	3660	symmetric OH stretch of the proton acceptor
D	3549	3547	3556	3588	hydrogen-bonded OH stretch of the proton donor
	3537				

Figure 3. Comparison of the experimental IR spectrum and calculated vibrational frequencies of water dimer in the OH stretching vibrational region. (a) Experimental spectrum measured in this study. (b) Calculated vibrational frequency based on a 12-dimensional ab initio potential energy surface (unscaled). (c) MP2/AVTZ harmonic vibrational frequency (scaled by 0.956). (d) CCSD(T)/AVTZ harmonic vibrational frequency (scaled by 0.961) (see the Supporting Information for details).

As shown in Figure 2, the experimental IR spectra of the water dimer comprise four groups of bands (labeled as A–D) and an extra band (labeled with "*"), which can be assigned by comparison with previous studies.[4,15,27,28,34,35] Band A is due to the antisymmetric OH stretch of the proton acceptor, which is rotationally resolved at 3764, 3780, and 3792 cm^{-1}. Band B (3732 cm^{-1}) is assigned to the free OH stretch of the proton donor, which is the most intense feature in the IR spectra. Band C at 3603 cm^{-1} is attributed to the symmetric OH stretch of the proton acceptor. The splitting of band D is observed at 3537 and 3549 cm^{-1}, which are assigned to the hydrogen-bonded OH stretch of the proton donor. The band labeled with "*" (3757 cm^{-1}) is observed with IR laser power of 6.6 mJ/mm^2 and disappears with IR laser powers of 2.0 and 3.3 mJ/mm^2. This asterisk-band differs from the features of bands A–D in that the band disappears when the power of IR laser is lowered, which indicates a combined or overtone excitation. As demonstrated before for the first overtone of the antisymmetric OH stretching in the infrared photodissociation spectra of $[MgNO_3(H_2O)_n]^+$ ($n = 1-3$),[42] the intensity of a higher-order excitation is more sensitive to the IR laser power. This asterisk-labeled band fits such a behavior very well, with its disappearance at low IR laser power, and is assigned to a combination or overtone band.

It is interesting to compare our results with previous measurements (Figure S1). The main features in the present spectrum are consistent with those in the previous studies.[4,15,28,34,35] In contrast with the general consensus in the work of Page, Coker, Huang, and Pribble et al.,[4,15,32−35] the major concern raised by Huisken et al. was that the ∼3600 cm^{-1} band was proposed to be hydrogen-bonded OH stretch of proton donor and the ∼3540 cm^{-1} band was presumed to originate from a water trimer.[28,32,33] Scenarios rationalizing this contradiction include the uncontrollable fragmentation owing to the electron impact ionization scheme used to detect the products. In our approach, the soft near-threshold ionization of the confinement-free water dimer avoids the extensive fragmentation and the complicatedness of ultraviolet chromophore tagging.

Quantum mechanical calculations were carried out with wave function theory at the MP2/aug-cc-pVTZ (AVTZ) and CCSD(T)/AVTZ levels with harmonic approximation and on a 12-dimensional (12D) ab initio potential energy surface to calculate the anharmonic vibrational spectra of the water dimer (see Theoretical Methods in the Supporting Information). Figure 3 shows the comparison of the experimental and calculated IR spectra. The harmonic and anharmonic vibra-

tional calculations reproduced the well-known four bands of the water dimer, which correspond to antisymmetric OH stretch of the proton acceptor (A), free OH stretch of the proton donor (B), symmetric OH stretch of the proton acceptor (C), and hydrogen-bonded OH stretch of the proton donor (D).

In the MP2/AVTZ calculated harmonic IR spectrum (Figure 3c and Table 1), the antisymmetric OH stretch of the proton acceptor is predicted at 3762 cm^{-1}, which is 18 cm^{-1} lower than the central position of experimental band A (3780 cm^{-1}); the free OH stretch of the proton donor is calculated to be 3743 cm^{-1}, which is in agreement with the experimental band B (3732 cm^{-1}); the symmetric OH stretch of the proton acceptor is calculated at 3646 cm^{-1}, which is 43 cm^{-1} higher than the experimental band C (3603 cm^{-1}); the hydrogen-bonded OH stretch of the proton donor is calculated to be 3556 cm^{-1}, which is consistent with the central position of the experimental band D. Similar results have also been obtained from the CCSD(T)/AVTZ calculations (Figure 3d and Table 1). The deviations of the harmonic MP2/AVTZ and CCSD(T)/AVTZ results from experimental values are due to the low-order electron correlation treatment with MP2 and CCSD(T), incomplete basis sets, and the harmonic approximation to potential energy surface.

The anharmonic calculations based on a 12D potential energy surface predict the bands A–D at 3766, 3716, 3640, and 3547 cm^{-1} (Figure 3b and Table 1), respectively, which improves the agreement with experiment. As shown in Figure 3, however, the splitting of bands A and D is not reproduced well in the calculated IR spectra likely because of vibrational anharmonic interactions, which can induce more observable vibrational transitions that otherwise are dark. In order to calculate the IR frequencies and intensities of the water dimer for more accurate comparison with experiment, the development of highly accurate electronic and vibrational description

of hydrogen bond potentials with rotational interactions are still needed.

The animation of vibrational normal modes of the four bands A−D of water dimer (represented as $HHO_a \cdots H-O_bH$) is given in the Supporting Information. The calculated bond distances, bond orders, natural hybrid orbitals, and natural localized molecular orbitals from the natural bond orbital (NBO) analysis[43] are listed in Table S3. As shown by the animation, the bands A and B are primarily the antisymmetric OH stretch mode of HHO_a and $H-O_bH$, respectively. Band C is the symmetric OH stretch mode of HHO_a coupled with slight contribution of $H-O_bH$, while band D is the symmetric OH stretch mode of $H-O_bH$ coupled with minor contribution of HHO_a. As shown by the bond distances, bond orders, and hybrid orbitals, the O−H bonds in HHO_a are stronger than those in the $H-O_bH$ because of electron donation from the O_a lone pair to the $\sigma(OH)^*$ antibonding orbitals,[44] and the symmetric and antisymmetric OH vibrational frequencies of HHO_a are higher than those of $H-O_bH$. The electronic structure analyses are helpful for understanding the spectroscopic features of OH vibrational modes for different hydrogen bond orientations in more complicated water clusters.

In summary, as compared to previous spectroscopy of neutral clusters, the advanced VUV-FEL-based IR spectroscopic method presented here allows (i) direct detection of confinement-free neutral complexes, (ii) near-threshold ionization with high sensitivity and size-selectivity, and (iii) recording of well-resolved vibrational spectra of size-selected neutral clusters. Because many clusters have their ionization energies in a range accessible by the VUV-FEL light source and near threshold ionization can be readily achieved, the VUV-FEL-based IR spectroscopy presents a new paradigm for the study of vibrational spectra of a wide variety of neutral clusters. The availability of these new experimental data on the neutral clusters is expected to stimulate further calculations and development of theoretical methods leading to an improved understanding of the structures and dynamics of these systems.

◼ ASSOCIATED CONTENT

Ⓢⓘ Supporting Information

The Supporting Information is available free of charge at https://pubs.acs.org/doi/10.1021/acs.jpclett.9b03683.

> Experimental and theoretical methods, Figures S1−S3, Tables S1−S3, and references (PDF)

> Animation of vibrational normal modes of the four bands A−D of water dimer (PPTX)

◼ AUTHOR INFORMATION

Corresponding Authors

Jun Li − *Tsinghua University, Beijing, China, and Southern University of Science and Technology, Shenzhen, China;* ⓞ orcid.org/0000-0002-8456-3980; Email: junli@tsinghua.edu.cn

Dong H. Zhang − *Dalian Institute of Chemical Physics, Dalian, China;* Email: zhangdh@dicp.ac.cn

Xueming Yang − *Dalian Institute of Chemical Physics, Dalian, China, and Southern University of Science and Technology, Shenzhen, China;* ⓞ orcid.org/0000-0001-6684-9187; Email: xmyang@dicp.ac.cn, yangxm@sustc.edu.cn

Ling Jiang − *Dalian Institute of Chemical Physics, Dalian, China;* ⓞ orcid.org/0000-0002-8485-8893; Email: ljiang@dicp.ac.cn

Other Authors

Bingbing Zhang − *Dalian Institute of Chemical Physics, Dalian, China*

Yong Yu − *Dalian Institute of Chemical Physics, Dalian, China, and University of Chinese Academy of Sciences, Beijing, China*

Zhaojun Zhang − *Dalian Institute of Chemical Physics, Dalian, China;* ⓞ orcid.org/0000-0002-4263-1789

Yang-Yang Zhang − *Tsinghua University, Beijing, China*

Shukang Jiang − *Dalian Institute of Chemical Physics, Dalian, China, and University of Chinese Academy of Sciences, Beijing, China*

Qinming Li − *Dalian Institute of Chemical Physics, Dalian, China, and University of Chinese Academy of Sciences, Beijing, China*

Shuo Yang − *Dalian Institute of Chemical Physics, Dalian, China, and University of Chinese Academy of Sciences, Beijing, China*

Han-Shi Hu − *Tsinghua University, Beijing, China*

Weiqing Zhang − *Dalian Institute of Chemical Physics, Dalian, China*

Dongxu Dai − *Dalian Institute of Chemical Physics, Dalian, China*

Guorong Wu − *Dalian Institute of Chemical Physics, Dalian, China;* ⓞ orcid.org/0000-0002-0212-183X

Complete contact information is available at:
https://pubs.acs.org/10.1021/acs.jpclett.9b03683

Author Contributions

[#]B.Z., Y.Y., Z.Z., and Y.-Y.Z. contributed equally to this work.

Notes

The authors declare no competing financial interest.

◼ ACKNOWLEDGMENTS

◼ REFERENCES

(1) Castleman, A. W.; Keesee, R. G. Clusters: Bridging the Gas and Condensed Phases. *Acc. Chem. Res.* **1986**, *19*, 413−419.

(2) Balle, T. J.; Flygare, W. H. Fabry-Perot Cavity Pulsed Fourier Transform Microwave Spectrometer with a Pulsed Nozzle Particle Source. *Rev. Sci. Instrum.* **1981**, *52*, 33−45.

(3) Vernon, M. F.; Lisy, J. M.; Krajnovich, D. J.; Tramer, A.; Kwok, H. S.; Shen, Y. R.; Lee, Y. T. Vibrational Predissociation Spectra and Dynamics of Small Molecular Clusters of H_2O and HF. *Faraday Discuss. Chem. Soc.* **1982**, *73*, 387−397.

(4) Huang, Z. S.; Miller, R. E. High-Resolution Near-Infrared Spectroscopy of Water Dimer. *J. Chem. Phys.* **1989**, *91*, 6613−6631.

(5) Buck, U.; Meyer, H. Scattering Analysis of Cluster Beams: Formation and Fragmentation of Small Ar_n Clusters. *Phys. Rev. Lett.* **1984**, *52*, 109−112.

(6) Goyal, S.; Schutt, D. L.; Scoles, G. Vibrational Spectroscopy of Sulfur Hexafluoride Attached to Helium Clusters. *Phys. Rev. Lett.* **1992**, *69*, 933−936.

(7) Pugliano, N.; Saykally, R. J. Measurement of Quantum Tunneling Between Chiral Isomers of the Cyclic Water Trimer. *Science* **1992**, *257*, 1937−1940.

(8) Diken, E. G.; Robertson, W. H.; Johnson, M. A. The Vibrational Spectrum of the Neutral $(H_2O)_6$ Precursor to the "Magic" $(H_2O)_6^-$ Cluster Anion by Argon-Mediated, Population-Modulated Electron Attachment Spectroscopy. *J. Phys. Chem. A* **2004**, *108*, 64−68.

(9) Brown, G. G.; Dian, B. C.; Douglass, K. O.; Geyer, S. M.; Shipman, S. T.; Pate, B. H. A Broadband Fourier Transform Microwave Spectrometer Based on Chirped Pulse Excitation. *Rev. Sci. Instrum.* **2008**, *79*, 053103.

(10) Page, R. H.; Shen, Y. R.; Lee, Y. T. Local Modes of Benzene and Benzene Dimer, Studied by Infrared−Ultraviolet Double Resonance in a Supersonic Beam. *J. Chem. Phys.* **1988**, *88*, 4621−4636.

(11) Woo, H. K.; Wang, P.; Lau, K. C.; Xing, X.; Chang, C.; Ng, C. Y. State-Selected and State-to-State Photoionization Study of Trichloroethene using the Two-Color Infrared-Vacuum Ultraviolet Scheme. *J. Chem. Phys.* **2003**, *119*, 9333−9336.

(12) Matsuda, Y.; Mori, M.; Hachiya, M.; Fujii, A.; Mikami, N. Infrared Spectroscopy of Size-Selected Neutral Clusters Combined with Vacuum-Ultraviolet-Photoionization Mass Spectrometry. *Chem. Phys. Lett.* **2006**, *422*, 378−381.

(13) Fu, H. B.; Hu, Y. J.; Bernstein, E. R. IR+Vacuum Ultraviolet (118 nm) Nonresonant Ionization Spectroscopy of Methanol Monomers and Clusters: Neutral Cluster Distribution and Size-Specific Detection of the OH Stretch Vibrations. *J. Chem. Phys.* **2006**, *124*, 024302.

(14) Normile, D. Unique Free Electron Laser Laboratory Opens in China. *Science* **2017**, *355*, 235−235.

(15) Pribble, R. N.; Zwier, T. S. Size-Specific Infrared Spectra of Benzene-$(H_2O)_n$ clusters (n = 1 through 7): Evidence for Noncyclic $(H_2O)_n$ Structures. *Science* **1994**, *265*, 75−79.

(16) Liu, K.; Cruzan, J. D.; Saykally, R. J. Water Clusters. *Science* **1996**, *271*, 929−933.

(17) Nauta, K.; Miller, R. E. Formation of Cyclic Water Hexamer in Liquid Helium: The Smallest Piece of Ice. *Science* **2000**, *287*, 293−295.

(18) Asmis, K. R.; Pivonka, N. L.; Santambrogio, G.; Brummer, M.; Kaposta, C.; Neumark, D. M.; Woste, L. Gas-phase Infrared Spectrum of the Protonated Water Dimer. *Science* **2003**, *299*, 1375−1377.

(19) Bragg, A. E.; Verlet, J. R. R.; Kammrath, A.; Cheshnovsky, O.; Neumark, D. M. Hydrated Electron Dynamics: From Clusters to Bulk. *Science* **2004**, *306*, 669−671.

(20) Miyazaki, M.; Fujii, A.; Ebata, T.; Mikami, N. Infrared Spectroscopic Evidence for Protonated Water Clusters Forming Nanoscale Cages. *Science* **2004**, *304*, 1134−1137.

(21) Shin, J. W.; Hammer, N. I.; Diken, E. G.; Johnson, M. A.; Walters, R. S.; Jaeger, T. D.; Duncan, M. A.; Christie, R. A.; Jordan, K. D. Infrared Signature of Structures Associated with the $H^+(H_2O)_n$ (n = 6 to 27) Clusters. *Science* **2004**, *304*, 1137−1140.

(22) Bukowski, R.; Szalewicz, K.; Groenenboom, G. C.; van der Avoird, A. Predictions of the Properties of Water from First Principles. *Science* **2007**, *315*, 1249−1252.

(23) Perez, C.; Muckle, M. T.; Zaleski, D. P.; Seifert, N. A.; Temelso, B.; Shields, G. C.; Kisiel, Z.; Pate, B. H. Structures of Cage, Prism, and Book Isomers of Water Hexamer from Broadband Rotational Spectroscopy. *Science* **2012**, *336*, 897−901.

(24) Pradzynski, C. C.; Forck, R. M.; Zeuch, T.; Slavicek, P.; Buck, U. A Fully Size-Resolved Perspective on the Crystallization of Water Clusters. *Science* **2012**, *337*, 1529−1532.

(25) Cole, W. T. S.; Farrell, J. D.; Wales, D. J.; Saykally, R. J. Structure and Torsional Dynamics of the Water Octamer from THz Laser Spectroscopy near 215 microm. *Science* **2016**, *352*, 1194−1197.

(26) Yang, N.; Duong, C. H.; Kelleher, P. J.; McCoy, A. B.; Johnson, M. A. Deconstructing Water's Diffuse OH Stretching Vibrational Spectrum with Cold Clusters. *Science* **2019**, *364*, 275−278.

(27) Xantheas, S. S.; Dunning, T. H. Ab Initio Studies of Cyclic Water Clusters $(H_2O)_n$ (n = 1−6). I. Optimal Structures and Vibrational Spectra. *J. Chem. Phys.* **1993**, *99*, 8774−8792.

(28) Huisken, F.; Kaloudis, M.; Kulcke, A. Infrared Spectroscopy of Small Size-Selected Water Clusters. *J. Chem. Phys.* **1996**, *104*, 17−25.

(29) Wang, Y.; Huang, X.; Shepler, B. C.; Braams, B. J.; Bowman, J. M. Flexible, Ab Initio Potential, and Dipole Moment Surfaces for Water. I. Tests and Applications for Clusters up to the 22-mer. *J. Chem. Phys.* **2011**, *134*, 094509.

(30) Leforestier, C.; Szalewicz, K.; van der Avoird, A. Spectra of Water Dimer from a New Ab Initio Potential with Flexible Monomers. *J. Chem. Phys.* **2012**, *137*, 014305.

(31) Clary, D. C. Quantum Dynamics in the Smallest Water Droplet. *Science* **2016**, *351*, 1267−1268.

(32) Keutsch, F. N.; Cruzan, J. D.; Saykally, R. J. The Water Trimer. *Chem. Rev.* **2003**, *103*, 2533−2577.

(33) Mukhopadhyay, A.; Cole, W. T. S.; Saykally, R. J. The Water Dimer I: Experimental Characterization. *Chem. Phys. Lett.* **2015**, *633*, 13−26.

(34) Page, R. H.; Frey, J. G.; Shen, Y. R.; Lee, Y. T. Infrared Predissociation Spectra of Water Dimer in a Supersonic Molecular Beam. *Chem. Phys. Lett.* **1984**, *106*, 373−376.

(35) Coker, D. F.; Miller, R. E.; Watts, R. O. The Infrared Predissociation Spectra of Water Clusters. *J. Chem. Phys.* **1985**, *82*, 3554−3562.

(36) Tachikawa, H. Ionization Dynamics of the Small-sized Water Clusters: A Direct Ab Initio Trajectory Study. *J. Phys. Chem. A* **2004**, *108*, 7853−7862.

(37) Belau, L.; Wilson, K. R.; Leone, S. R.; Ahmed, M. Vacuum Ultraviolet (VUV) Photoionization of Small Water Clusters. *J. Phys. Chem. A* **2007**, *111*, 10075−10083.

(38) Garrett, B. C.; et al. Role of Water in Electron-Initiated Processes and Radical Chemistry: Issues and Scientific Advances. *Chem. Rev.* **2005**, *105*, 355−389.

(39) Matsuda, Y.; Mikami, N.; Fujii, A. Vibrational Spectroscopy of Size-Selected Neutral and Cationic Clusters Combined with Vacuum-Ultraviolet One-Photon Ionization Detection. *Phys. Chem. Chem. Phys.* **2009**, *11*, 1279−1290.

(40) Rocher-Casterline, B. E.; Ch'ng, L. C.; Mollner, A. K.; Reisler, H. Determination of the Bond Dissociation Energy (D_0) of the Water Dimer, $(H_2O)_2$, by Velocity Map Imaging. *J. Chem. Phys.* **2011**, *134*, 211101.

(41) Shank, A.; Wang, Y.; Kaledin, A.; Braams, B. J.; Bowman, J. M. Accurate Ab Initio and "Hybrid" Potential Energy Surfaces, Intramolecular Vibrational Energies, and Classical IR Spectrum of the Water Dimer. *J. Chem. Phys.* **2009**, *130*, 144314.

(42) Jiang, L.; Wende, T.; Bergmann, R.; Meijer, G.; Asmis, K. R. Gas-Phase Vibrational Spectroscopy of Microhydrated Magnesium Nitrate Ions $MgNO_3(H_2O)_{1−4}^+$. *J. Am. Chem. Soc.* **2010**, *132*, 7398−7404.

(43) Weinhold, F.; Landis, C. R.; Glendening, E. D. What Is NBO Analysis and How Is It Useful? *Int. Rev. Phys. Chem.* **2016**, *35*, 399−440.

(44) Reed, A. E.; Weinhold, F. Natural Bond Orbital Analysis of Near-Hartree-Fock Water Dimer. *J. Chem. Phys.* **1983**, *78*, 4066−4073.